

## $^{98}_{48}\text{Cd}_{50}$ : The Two-Proton-Hole Spectrum in $^{100}_{50}\text{Sn}_{50}$

M. Górska,<sup>1,2</sup> M. Lipoglavšek,<sup>3,4</sup> H. Grawe,<sup>1,5</sup> J. Nyberg,<sup>3</sup> A. Ataç,<sup>3</sup> A. Axelsson,<sup>3</sup> R. Bark,<sup>6</sup> J. Blomqvist,<sup>7</sup> J. Cederkäll,<sup>7</sup> B. Cederwall,<sup>7</sup> G. de Angelis,<sup>8</sup> C. Fahlander,<sup>3,8</sup> A. Johnson,<sup>7</sup> S. Leoni,<sup>6</sup> A. Likar,<sup>4</sup> M. Matiuuzzi,<sup>6</sup> S. Mitarai,<sup>9</sup> L.-O. Norlin,<sup>7</sup> M. Palacz,<sup>10</sup> J. Persson,<sup>3</sup> H. A. Roth,<sup>11</sup> R. Schubart,<sup>1</sup> D. Seweryniak,<sup>12,13</sup> T. Shizuma,<sup>9</sup> Ö. Skeppstedt,<sup>11</sup> G. Sletten,<sup>6</sup> W. B. Walters,<sup>13</sup> and M. Weiszflog<sup>3</sup>

<sup>1</sup>*Gesellschaft für Schwerionenforschung, Planckstrasse 1, D-64291 Darmstadt, Germany*

<sup>2</sup>*Institute of Experimental Physics, University of Warsaw, Warsaw, Poland*

<sup>3</sup>*The Svedberg Laboratory and Department of Radiation Sciences, Uppsala University, Uppsala, Sweden*

<sup>4</sup>*J. Stefan Institute, Ljubljana, Slovenia*

<sup>5</sup>*Hahn-Meitner Institute, Berlin, Germany*

<sup>6</sup>*Niels Bohr Institute, University of Copenhagen, Copenhagen, Denmark*

<sup>7</sup>*Department of Physics, Royal Institute of Technology, Stockholm, Sweden*

<sup>8</sup>*INFN, Laboratori Nazionali di Legnaro, Legnaro (Padova), Italy*

<sup>9</sup>*Department of Physics, Faculty of Science, Kyushu University, Fukuoka, Japan*

<sup>10</sup>*Soltan Institute for Nuclear Studies, Świerk, Poland*

<sup>11</sup>*Chalmers University of Technology, Gothenburg, Sweden*

<sup>12</sup>*Argonne National Laboratory, Argonne, Illinois*

<sup>13</sup>*Department of Chemistry, University of Maryland, College Park, Maryland*

(Received 18 December 1996)

Excited states in  $^{98}\text{Cd}$ , two proton holes from  $^{100}\text{Sn}$ , were identified and studied for the first time, using in-beam spectroscopy with highly selective ancillary detectors. The structure of the  $(\pi g_{9/2})^{-2}$  two-proton-hole spectrum below a  $T_{1/2} = 0.48(16) \mu\text{s}$  isomer is deduced and compared to shell-model predictions. A tentative  $I^\pi = (8^+)$  assignment, as suggested by systematics, yields a strongly reduced  $B(E2, 8^+ \rightarrow 6^+) = 0.44(^{+20}_{-10}) \text{ W.u.}$ , corresponding to an effective proton charge of  $e_\pi = 0.85(^{+20}_{-10})e$ , which is at variance with existing theoretical predictions. [S0031-9007(97)04116-1]

PACS numbers: 21.10.Tg, 21.60.Cs, 23.20.Lv, 27.60.+j

The  $N = Z$  nucleus  $^{100}\text{Sn}$ , recently observed in a few events [1,2], is the heaviest doubly magic  $T_z = 0$  nucleus, where shell closure, single-particle energies, and residual interaction can be studied experimentally. The closest approach so far to  $^{100}\text{Sn}$  in  $\gamma$ -ray spectroscopy of excited states is landmarked by the  $T_z = 2$  nuclei  $^{96}\text{Pd}_{50}$  to  $^{104}\text{Sn}_{54}$  [3–6], the  $T_z = 3/2$  nuclei  $^{97}\text{Ag}_{50}$  to  $^{101}\text{In}_{52}$  [7–9], and the  $T_z = 1$  nuclei  $^{98}\text{Cd}_{50}$  (this work) and  $^{102}\text{Sn}_{52}$  [10]. Experimental investigations of  $^{100}\text{Sn}$  and its one- and two-particle (hole) neighbors provide the unique chance to study the mean field and residual interactions in isospin symmetric nuclear matter. Besides  $^{56}\text{Ni}$ , the double shell closure at  $N = Z = 50$  is the only one with an open  $ls$  core for both protons and neutrons in identical orbits, allowing strong  $E2$  particle-hole excitations, enhanced by proton ( $\pi$ )-neutron ( $\nu$ ) interaction. Implications for a low-energy  $I^\pi = 2^+$  state in  $^{100}\text{Sn}$  and  $E2$  softness, as observed in  $^{56}\text{Ni}$ , have been discussed controversially [4,8] with respect to  $E2$  polarization charges for protons and neutrons. Detailed knowledge of the microscopic structure of the nuclei in the vicinity of  $^{100}\text{Sn}$  is an indispensable prerequisite to understanding  $\pi\nu$  pairing [11], Gamow-Teller decay [12], and isospin mixing [13].

In two experiments, we studied the level structure of the  $T_z = 1$  nuclides  $^{98}\text{Cd}$  and  $^{102}\text{Sn}$  [10]. The experiments were performed at the Tandem Accelerator Laboratory of the Niels Bohr Institute in Risø. A  $^{58}\text{Ni}$  beam

with energies 215 and 225 MeV was used to bombard 1 mg/cm<sup>2</sup> thick targets of  $^{46}\text{Ti}$ , enriched to 86% (with 11%  $^{48}\text{Ti}$ ), and  $^{50}\text{Cr}$ , enriched to 99%, respectively. As a long-lived isomeric state was expected in  $^{98}\text{Cd}$  [14,15], a special detector setup was designed to maximize the sensitivity for delayed  $\gamma$  rays in coincidence with light particles emitted from the compound nucleus. Around the target, parts of the NORDBALL detector system consisting of a new version of the  $4\pi$  silicon ball [16] with 31 segments of  $\Delta E$  detectors, a  $2\pi$  neutron wall with 15 liquid scintillators [17], and 5 large  $\text{BaF}_2$  crystals were assembled allowing for reaction exit channel identification and serving as a precise time reference. Two EUROBALL Ge cluster detectors [18] were mounted in close geometry around an exchangeable Nb recoil catcher foil 60 cm downstream from the target, where the evaporation residues were stopped after about 50 ns time of flight. The  $\gamma$ -ray photopeak efficiency was about 6% at 1.3 MeV and the detection efficiencies for protons,  $\alpha$  particles, and neutrons were 64%, 42%, and 30%, respectively. By placing the catcher foils downstream from the target, and exchanging them periodically, prompt and  $\beta$ -delayed  $\gamma$  rays were largely suppressed. Further experimental details are given in Ref. [10].

In Fig. 1  $\gamma$ -ray spectra obtained for various particle gates are shown. In the  $\alpha 2n$  spectrum [Fig. 1(a)] besides the well known 1415 keV  $2^+ \rightarrow 0^+$   $\gamma$  ray in

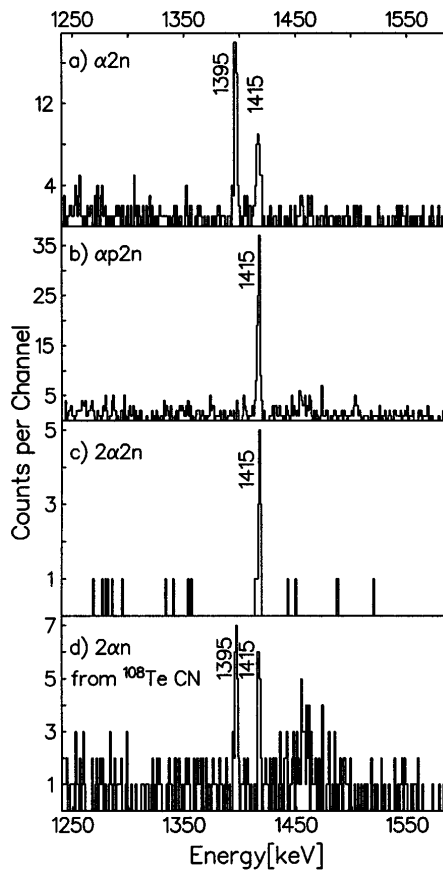


FIG. 1. Gamma-ray spectra gated with different particle folds as indicated in the figure. Spectra (a), (b), and (c) show data from the  $^{58}\text{Ni} + ^{46}\text{Ti}$  reaction and spectrum (d) corresponds to the  $^{58}\text{Ni} + ^{50}\text{Cr}$  reaction.

$^{96}\text{Pd}$ , populated in  $^{46,48}\text{Ti}(^{58}\text{Ni}, \alpha 2p 2n / 2\alpha 2n)$  reactions, a new line at 1395 keV is observed. It disappears in coincidence with a proton [Fig. 1(b)] or an additional  $\alpha$  particle [Fig. 1(c)], which determines the exit channel to  $^{46}\text{Ti}(^{58}\text{Ni}, \alpha 2n)^{98}\text{Cd}$ . The neutron multiplicity  $M_n$  associated with the 1395 keV transition was deduced from the intensity ratio  $I_{2n\gamma}/I_{n\gamma}$  of  $2n$  and  $1n$  gated  $\gamma$ -ray spectra for this line and the 1005 keV transition in  $^{100}\text{Cd}$  that is produced in a  $2p 2n$  exit channel. The ratios were 0.24(4) and 0.20(1), respectively, which establishes  $M_n = 2$ . The 1395 keV line was also observed in the  $2\alpha 2n$  exit channel from the  $^{58}\text{Ni} + ^{50}\text{Cr}$  reaction [Fig. 1(d)], which excludes a possible misidentification due to carbon and oxygen target contamination. Three other  $\gamma$  rays at 147, 198, and 688 keV were found to be in mutual coincidence with the 1395 keV transition [Fig. 2(a)] suggesting the level scheme shown in Fig. 3. All  $\gamma$  rays are delayed with an apparent half-life of 0.48(16)  $\mu\text{s}$  as determined from an exponential fit to the time distributions of the two high energy lines at 688 and 1395 keV [Fig. 2(b)]. The individual half-life results fitted for the 147 and 198 keV transitions agree with this value within 0.15  $\mu\text{s}$ .

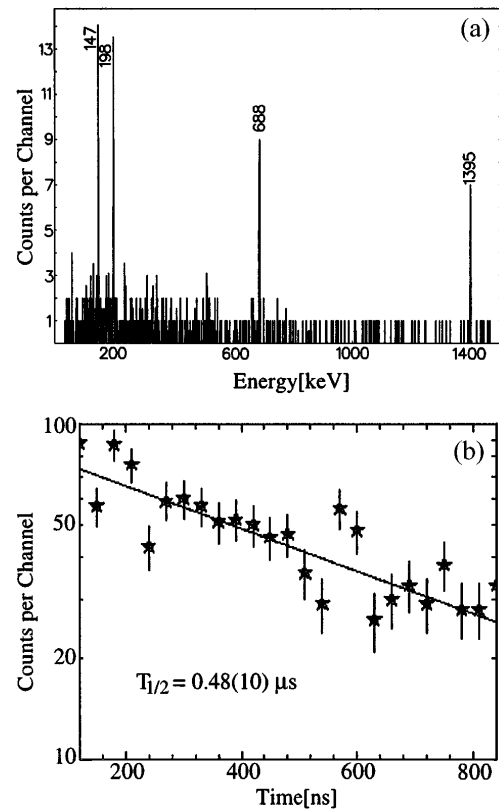


FIG. 2. (a) Sum coincidence spectrum obtained from the  $\alpha 1n$  and  $\alpha 2n$  gated  $\gamma$ - $\gamma$  matrices. (b) Sum of the time spectra of the 688 and 1395 keV transitions gated with the  $1n$ ,  $2n$ ,  $\alpha 1n$ , and  $\alpha 2n$  particle conditions. The statistical error of  $T_{1/2}$  is given.

The level sequence and spin and parity assignments for  $^{98}\text{Cd}$  were taken from the systematics of the  $N = 50$  isotones (Fig. 3). They are supported by the  $\gamma$ -ray intensities given in Table I and the conversion factor  $\alpha_t(147 \text{ keV}) = 0.35(23)$ .

An  $I^\pi = (8^+)$  assignment along with the measured half-life has spectacular implications for the  $B(E2; 8^+ \rightarrow 6^+)$  and the extracted proton effective charge, as discussed below. Therefore an alternative  $5^-$  assignment, a state which is observed at this energy in the  $N = 50$  isotones [19,20] and predicted in shell-model calculations (Fig. 3), or the existence of a core excited isomer as known in  $^{96}\text{Pd}$  [19] were studied, assuming the following scenarios.

(i) *The isomer is an  $I^\pi = (5^-)$  state with  $B(E1; 5^- \rightarrow 6^+) = 2.8^{(+1.4)}_{(-0.7)} \times 10^{-7}$  W.u.* This is 50 times weaker than the lower limit  $B(E1) > 2.1 \times 10^{-5}$  W.u. [20] of three measured  $5^- \rightarrow 6^+$  transitions in the  $N = 50$  isotones  $^{90}\text{Zr}$ - $^{96}\text{Pd}$ . From these nuclei a minimum branch  $I_\gamma(5^- \rightarrow 4^+; 345 \text{ keV}) > 35\%$  is expected for  $^{98}\text{Cd}$ , which is not seen in Fig. 2(a). Also the conversion coefficient  $\alpha_t(147 \text{ keV})$  (Table I) and the nonobservation of the  $8^+$  isomer, which in  $^{94}\text{Ru}$  and  $^{96}\text{Pd}$  is populated 10 times stronger than the  $5^-$  state, are at variance with a  $5^-$  assignment.

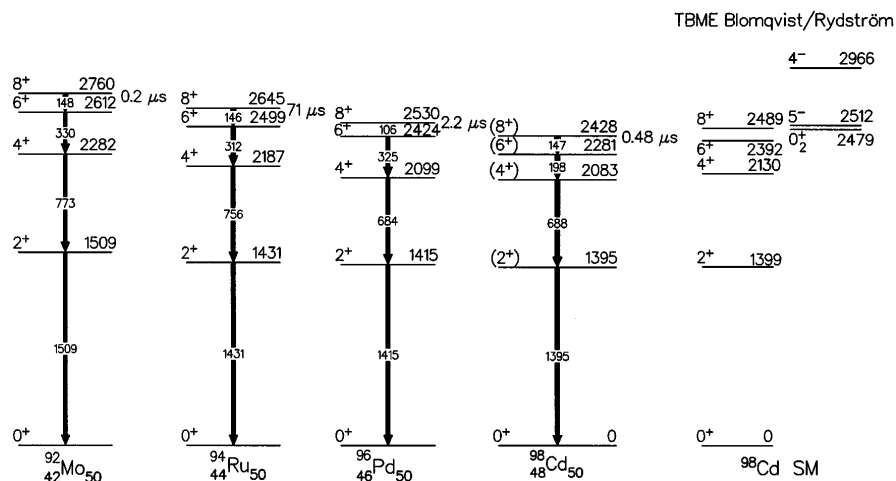


FIG. 3. Proposed experimental level scheme of  $^{98}\text{Cd}$  in comparison to  $N = 50$  isotones (left) and shell-model predictions (right).

(ii) The  $8^+ \rightarrow 6^+$   $\gamma$  ray is unobserved ( $E_\gamma < 80$  keV), while a  $5^- \rightarrow 6^+$  transition from a  $5^-$  isomer of comparable half-life is seen. This would be consistent with the large errors of about 150 ns on the lifetime values determined for the two low energy transitions, but again is at variance with the intensity balance in the cascade,  $\alpha_i(147$  keV) and nonobservation of a  $5^- \rightarrow 4^+$ ; 345 keV branch.

(iii) There is a core excited isomer above the  $8^+$  isomer determining the half-life. This requires nonobservation of at least two more  $\gamma$  rays outside the dynamic range of  $80$  keV  $< E_\gamma < 3.0$  MeV. Because of the large difference in excitation energy one would expect an appreciable side feeding of the  $8^+$  isomer and a short-lived component in the time spectrum of Fig. 2(b).

In conclusion an  $I^\pi = 8^+$  assignment to the isomer is most probable, but in view of the statistical uncertainties and in spite of the carefully selected  $E1$  systematics an  $I^\pi = 5^-$  assignment or the existence of a core excited isomer of unknown spin cannot be definitely excluded.

Based on the tentative  $I^\pi = 8^+$  assignment and assuming pure  $g_{9/2}^{-2}$  configurations for the  $I^\pi = (4^+) - (8^+)$  states (see discussion below), the existence of a second isomeric lifetime in the  $I^\pi = (6^+)$  state is expected. From shell-model recoupling techniques, regarding transition energies and conversion factors, this is given by the fixed ratio  $T_{1/2}(8^+)/T_{1/2}(6^+) = 8.85$ . A two level expo-

ponential fit with this restriction yields the model dependent corrected value of  $T_{1/2}(8^+) = 0.41(14)$   $\mu\text{s}$ . The lifetime measurement, background subtraction, and fitting procedure were checked by analyzing the time distribution of the equally weak 1415 keV  $\gamma$  ray in  $^{96}\text{Pd}$  (see Fig. 1), yielding a value of  $T_{1/2} = 2.1(5)$   $\mu\text{s}$  in good agreement with the known value [14]. This uncertainty of 25%, as a conservative estimate of systematic errors, is included in the  $^{98}\text{Cd}$  value. From a comparison of the  $\gamma\gamma$  coincidence intensities to the well known  $^{100}\text{Cd}$  nucleus [5,22], which was strongly populated in the present experiment, the production cross section was determined to be  $20(10)$   $\mu\text{b}$ . Intensities were corrected for  $\gamma$ -ray and particle detection efficiencies, assuming that in  $^{98}\text{Cd}$  100% of the  $\gamma$ -ray flux is following the isomeric path.

The level systematics of the predominantly  $(\pi g_{9/2})^{-n}$  states shown in Fig. 3 resembles very much the  $(\pi h_{9/2})^n$  states of the  $N = 126$  isotones above  $^{208}\text{Pb}$  [23]. Because of increased pair correlations, the excitation energies of the  $I^\pi = 2^+$  and the stretched two-quasi-particle states with  $I^\pi = 8^+$  increase relative to the ground state when moving from the doubly magic nucleus into the open proton shell [23]. This is also observed in the  $(\pi g_{7/2})^n$  states of the  $N = 82$  isotones above  $^{132}\text{Sn}$  [24]. In a shell-model calculation that uses the parametrization by Blomqvist and Rydström of the  $\pi(p_{1/2}, g_{9/2})$  model space [25], which is shown on the right hand side of Fig. 3, only the ground state has a mixed  $\pi p_{1/2}^2 g_{9/2}^8$  (87%) and  $\pi g_{9/2}^{10}$  (13%) wave function. The excited states of  $^{98}\text{Cd}$  represent the pure  $(\pi g_{9/2})^{-2}$  two-proton-hole spectrum in  $^{100}\text{Sn}$ . A closer inspection of the minor deviations between shell-model predictions and experiment reveals that only the  $I^\pi = 4^+, 6^+$ , and  $8^+$  two-body matrix elements need to be corrected to deduce the true  $(\pi g_{9/2})^{-2}$  spectrum in  $^{100}\text{Sn}$ .

Concerning the recently emphasized shell structure similarities between  $^{56}\text{Ni}$  and  $^{100}\text{Sn}$  [26], we note that the

TABLE I. Relative  $\gamma$ -ray intensities in  $^{98}\text{Cd}$ .

$E_\gamma$ (keV)	$I_\gamma$	$I_{\text{tot}}$	Experiment	$\alpha_i$ E2 [21]	E1 [21]
147.3(3)	75(10)	103(14)	0.35(23)	0.375	0.055
197.9(3)	87(11)	99(13)	0.16(18)	0.137	0.025
687.6(3)	102(15)	102(15)			
1394.7(3)	100(15)	100(15)			

excitation energies of the first excited  $I^\pi = 2^+$  states for the two-, four-, and six-particle (hole) isotopes (isotones) of  $^{100}\text{Sn}$  and  $^{56}\text{Ni}$  agree within an rms deviation of 60 keV. It is tempting to predict from this the existence of a  $2^+$  state in  $^{100}\text{Sn}$  at 2.7 MeV as known in  $^{56}\text{Ni}$  [27].

Despite the good shell-model description of level schemes of the  $N = 50$  isotones in the  $\pi(p_{1/2}, g_{9/2})$  model space using empirical interactions [25,28,29], a breakdown in the systematics of the  $B(E2; 8^+ \rightarrow 6^+)$  strengths is observed above  $^{96}\text{Pd}$ , if the  $I^\pi = 8^+$  assignment is adopted for  $^{98}\text{Cd}$ . From  $^{90}\text{Zr}$  to  $^{96}\text{Pd}$ , except for the weak transitions in the midshell nuclei  $^{94}\text{Ru}$  and  $^{95}\text{Rh}$ , the  $E2$  strengths are well reproduced with an effective proton charge of  $e_\pi = 1.72e$  [3,4,30], as deduced from selected states of high configurational purity around  $^{90}\text{Zr}$  [31]. The deduced value for  $^{98}\text{Cd}$ ,  $B(E2; 8^+ \rightarrow 6^+) = 0.44 \binom{+20}{-10}$  W.u., corresponds to an effective charge of only  $e_\pi = 0.85 \binom{+20}{-10}e$ , when harmonic oscillator wave functions with  $b = (\hbar/M\omega)^{1/2} = 2.17$  fm are used. This  $e_\pi$  value would be increased by 7%, when the model dependent corrected half-life is used. This is to be compared with  $e_\pi = 1.3(3)e$  deduced for pure  $g_{9/2}^{-3}$  states in  $^{97}\text{Ag}$  [7] and with theoretical predictions of a proton effective charge  $e_\pi = 1.6\text{--}2.0e$  [32,33]. Recent results on states of mixed proton-neutron structure in  $^{99}\text{Cd}$  [8] and  $^{94}\text{Pd}$  [26] are contradictory ( $e_\pi \approx 1.6$  and  $1.0$ , respectively) and ambiguous, as  $e_\pi$  and  $e_\nu$  can compensate each other to a high degree. On the other hand fairly large neutron effective charges are required to explain the observed  $B(E2; 6^+ \rightarrow 4^+)$  in  $^{102}\text{Sn}$  ( $e_\nu \geq 1.3e$ ) [10] and  $^{104}\text{Sn}$  ( $e_\nu \approx 2.0e$ ) in large scale shell-model calculations [4,34], while the theoretically predicted effective charge is  $e_\nu \approx 0.8$  [32,33]. The opposite trends of  $e_\pi$  and  $e_\nu$  indicate an unusually large isovector polarization charge  $e_{IV} = \frac{1}{2}(e_\nu - e_\pi + 1) > 0.6$ , taking the lower limit for  $e_\nu$  from  $^{102}\text{Sn}$  and the upper limit for  $e_\pi$  from  $^{98}\text{Cd}$ .

Explanations for this inferred result have to account for the isovector character and the deviation in comparison to  $^{56}\text{Ni}$ , which in its shell structure is very similar to  $^{100}\text{Sn}$  [3]. This rules out an isoscalar proton-neutron interaction, which would increase both  $e_\pi$  and  $e_\nu$ . The asymmetry in proton-neutron structure introduced by large Coulomb shifts, the close lying proton dripline, and the different single particle structure of proton holes and neutron particles is therefore most likely the origin of the unexpected result. Clearly a quantitative analysis requires a more detailed study of core excited states around  $^{100}\text{Sn}$ , and a consistent theoretical treatment of the

proton-neutron interaction at  $N \approx Z$  and the influence of excitations into loosely bound states beyond the  $Z = 50$  shell closure.

- 
- [1] R. Schneider *et al.*, *Z. Phys. A* **348**, 241 (1994).
  - [2] M. Lewitowicz *et al.*, *Phys. Lett. B* **332**, 20 (1994).
  - [3] H. Grawe *et al.*, *Phys. Scr.* **T56**, 71 (1995).
  - [4] R. Schubart *et al.*, *Z. Phys. A* **352**, 373 (1995).
  - [5] D. Alber *et al.*, *Z. Phys. A* **344**, 1 (1992).
  - [6] D. Seweryniak *et al.*, *Z. Phys. A* **345**, 243 (1993).
  - [7] D. Alber *et al.*, *Z. Phys. A* **335**, 265 (1990).
  - [8] M. Lipoglavšek *et al.*, *Phys. Rev. Lett.* **76**, 888 (1996).
  - [9] J. Cederkäll *et al.*, *Phys. Rev. C* **53**, 1955 (1996).
  - [10] M. Lipoglavšek *et al.*, *Z. Phys. A* **356**, 239 (1996).
  - [11] W. Nazarewicz, J. Dobaczewski, and T. Werner, *Phys. Scr.* **T56**, 9 (1995).
  - [12] K. Rykaczewski, *Inst. Phys. Conf. Ser.* **132**, 517 (1993).
  - [13] J. Dobaczewski and I. Hamamoto, *Phys. Lett. B* **345**, 181 (1995).
  - [14] H. Grawe and H. Haas, *Phys. Lett.* **120B**, 63 (1983).
  - [15] R. Grzywacz *et al.*, *Phys. Rev. C* **55**, 1126 (1997).
  - [16] T. Kuroyanagi *et al.*, *Nucl. Instrum. Methods Phys. Res., Sect. A* **316**, 289 (1992).
  - [17] S. E. Arnell *et al.*, *Nucl. Instrum. Methods Phys. Res., Sect. A* **300**, 303 (1991).
  - [18] M. Wilhelm *et al.*, *Nucl. Instrum. Methods Phys. Res., Sect. A* **381**, 462 (1996), and references therein.
  - [19] D. Alber *et al.*, *Z. Phys. A* **332**, 129 (1989).
  - [20] F. K. Tuli, *Nucl. Data Sheets* **66**, 1 (1992); C. M. Baglin, *Nucl. Data Sheets* **66**, 347 (1992); L. P. Ekström and J. Lyttkens-Linden, *Nucl. Data Sheets* **67**, 579 (1992); L. K. Peker, *Nucl. Data Sheets* **68**, 165 (1993).
  - [21] F. Rösel *et al.*, *Nucl. Data Tables* **21**, 91 (1978).
  - [22] M. Gorska *et al.*, *Z. Phys. A* **350**, 181 (1994).
  - [23] D. Decman *et al.*, *Nucl. Phys.* **A436**, 311 (1985).
  - [24] K. Kawade *et al.*, *Z. Phys. A* **298**, 187 (1980), and references therein.
  - [25] J. Blomqvist and L. Rydström, *Phys. Scr.* **31**, 31 (1985).
  - [26] H. Grawe *et al.*, *Prog. Part. Nucl. Phys.* (to be published).
  - [27] G. Kraus *et al.*, *Phys. Rev. Lett.* **73**, 1773 (1994).
  - [28] R. Gross and A. Frenkel, *Nucl. Phys.* **A267**, 85 (1976).
  - [29] D. H. Gloeckner and F. J. D. Serduke, *Nucl. Phys.* **A220**, 477 (1974).
  - [30] H. Grawe *et al.*, in *Proceedings of the International Workshop on Nuclear Structure of the Zirconium Region, Bad Honnef, 1988* (Springer-Verlag, Berlin, 1989), p. 269.
  - [31] P. Raghavan *et al.*, *Phys. Rev. Lett.* **54**, 2592 (1985).
  - [32] J. Sinatkas *et al.*, *J. Phys. G* **18**, 1377, 1401 (1992).
  - [33] I. Hamamoto and H. Sagawa, *Phys. Lett. B* **394**, 1 (1997).
  - [34] F. Andreatti *et al.*, *Phys. Rev. C* **54**, 1636 (1996).